# Monte Carlo radiative transfer

## Non-Flat Probability Distribution Sampling

To sample values of $\mu = \cos\theta$ from the non-uniform distribution

$$P(\mu)\,d\mu = \frac{3}{8}(1+\mu^2)\,d\mu,$$

I implemented two methods in `C`, using a custom minimal standard generator (`msg`). Both using 1,000,000 points. The first method was **rejection sampling**. I swept through the domain $\mu \in [-1, 1]$ in fixed steps and accepted points based on comparing a uniform random value to the probability $P(\mu)$. Accepted samples were plotted alongside the theoretical distribution in the first graph, showing a good visual match despite the method's **66.69% efficiency**.

The second method was **inverse transform sampling**, which required deriving the cumulative distribution function (CDF) of $P(\mu)$. I analytically integrated the function:

$$\int_0^x P(\mu)\,d\mu = \int_0^x \frac{3}{8}(1+\mu^2)\,d\mu = \frac{3}{8}\left(x + \frac{x^3}{3}\right),$$

and then solved this expression for $x$ in terms of a uniform variable $y \in [0, 1]$ to construct the inverse CDF. Since this only yields positive $x$, I randomly flipped the sign of each sample with a 50% probability (by checking whether a second random seed was even or odd) to fully cover $\mu \in [-1, 1]$.

The resulting samples, shown in the second plot as a histogram, closely follow the theoretical distribution curve. This method achieved **100% efficiency** and completed faster than rejection sampling, clearly illustrating its advantage.

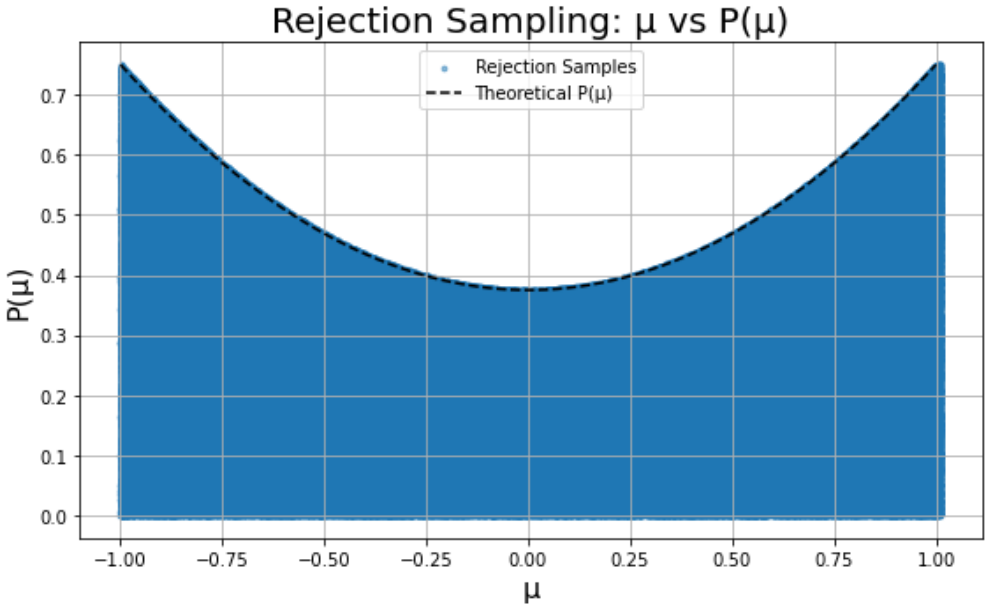


Figure 1: Rejection sampling: Random samples of $\mu$ plotted against the theoretical distribution $P(\mu) = \frac{3}{8}(1+\mu^2)$. Points lie below the curve, showing accepted values. Sampling efficiency was 66.69%.

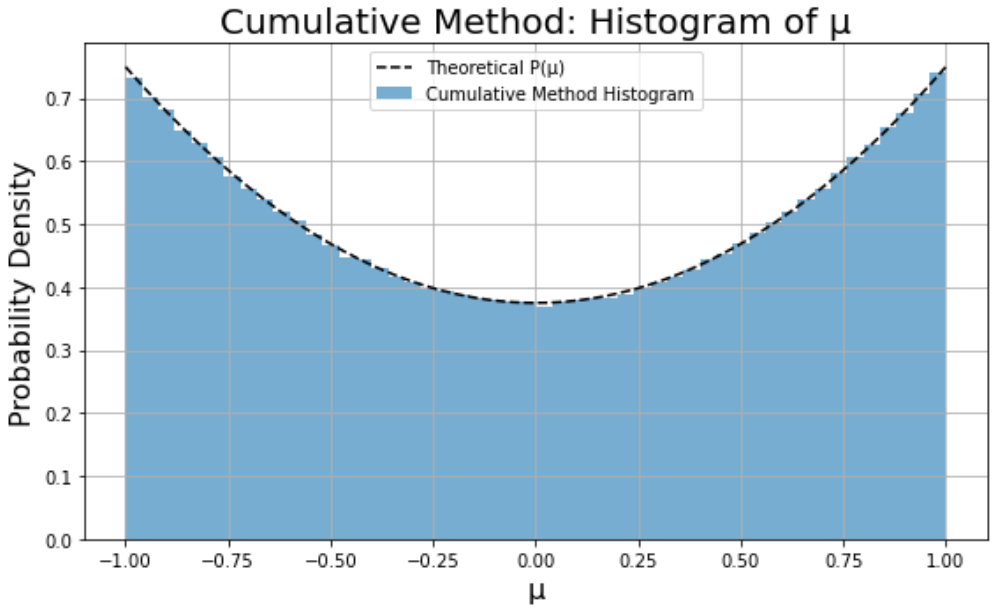


Figure 2: Inverse transform sampling: Histogram of sampled $\mu$ values closely matches the theoretical distribution. Sampling efficiency was 100%, demonstrating the improved performance of this method.

## Q2a: Monte Carlo Slab Scattering — Isotropic

To simulate isotropic Monte Carlo radiative transfer through an atmosphere, I modeled a slab geometry extending from $z_{\min} = 0$ to $z_{\max} = 200$, with a total optical depth $\tau = 10$ in the vertical direction. The slab is infinite in the $x$–$y$ plane and has a constant absorption coefficient

$$\alpha_\nu = \frac{\tau}{z_{\max} - z_{\min}} = \frac{10}{200} = 0.05.$$

I launched $10^6$ photons from the origin at $(x, y, z) = (0, 0, 0)$, each with normalized energy $h\nu = 1$. Initial directions were sampled isotropically by drawing a random number $y \in [0, 1]$ and computing $\mu = \cos\theta = 1 - 2y$, along with an azimuthal angle $\phi \in [0, 2\pi)$. Cartesian displacements were computed using:

$$dx = l \sin\theta \cos\phi, \quad dy = l \sin\theta \sin\phi, \quad dz = l \cos\theta,$$

where the photon free path length was drawn from the exponential distribution: $\tau_s = -\ln(y)$, and $l = \tau_s/\alpha_\nu$.

Although absorption was disabled (albedo $a = 1$), I implemented a dummy conditional check using a uniform random variable to determine whether the photon would scatter or be absorbed. Currently, the photon always scatters.

Each photon was tracked through successive scattering events until it either exited the slab at $z > z_{\max}$, or was discarded if it escaped downward past the base of the atmosphere ($z < z_{\min}$).

Escaping photons were binned based on their final direction cosine $\mu = \cos\theta$, using 10 equal-sized solid angle bins. I used int index = (int)(($\mu$ + 1.0) * $N_{\text{bins}}$ / 2.0) to map each escaping direction into its appropriate bin. Intensities were normalized by dividing bin counts by the total number of photons.

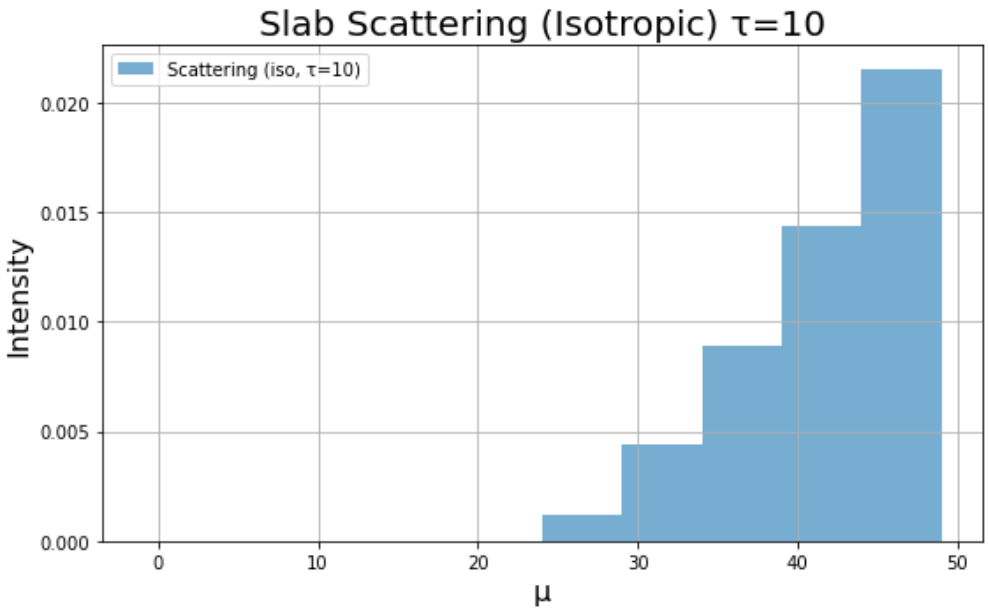


Figure 3: Histogram of outgoing photon intensity versus $\mu = \cos\theta$ for isotropic scattering in a slab with $\tau = 10$. Intensity increases with $\mu$, indicating that most photons escape in near-vertical directions after multiple scatterings.

## Q3: Rayleigh Scattering and the Colour of the Sky

To simulate Rayleigh scattering, I modified the isotropic scattering setup to instead sample scattering angles from the Rayleigh phase function:

$$P(\hat{\theta})\, d\Omega = \frac{3}{4}(1 + \cos^2\hat{\theta}) \cdot \frac{d\Omega}{4\pi},$$

where $\hat{\theta}$ is the angle between the incoming and outgoing photon directions.

I launched photons vertically upwards from the origin with initial direction vector $\mathbf{d}_0 = (0, 0, 1)$, and used inverse transform sampling to sample values of $\mu = \cos\hat{\theta}$ from the marginal distribution:

$$P(\mu) = \frac{3}{8}(1 + \mu^2).$$

The inverse CDF was used to generate positive $\mu$, and I randomly flipped the sign of each value with 50% probability to fully sample the domain $\mu \in [-1, 1]$.

To scatter the photon in the correct direction, I constructed an orthonormal frame from the current direction vector. A perpendicular vector $\mathbf{n}$ was found (analytically chosen based on whether $\mathbf{d}_z$ was close to $\pm 1$), and a third orthogonal vector $\mathbf{v} = \mathbf{d} \times \mathbf{n}$ was computed. The new direction vector was then given by:

$$\mathbf{d}' = \sin\theta\cos\phi\,\mathbf{n} + \sin\theta\sin\phi\,\mathbf{v} + \cos\theta\,\mathbf{d},$$

and normalized. This effectively rotated the scattering angle $\hat{\theta}$ relative to the incoming direction into the lab frame.

Photons were tracked until they exited the slab at $z > z_{\max} = 200$, or were discarded if they went below $z_{\min} = 0$. Escaping photons were binned in 10 equal-solid-angle bins based on their final escape angle cosine $\mu = \cos\theta$. Two separate simulations were run with $\tau = 10$ and $\tau = 0.1$.

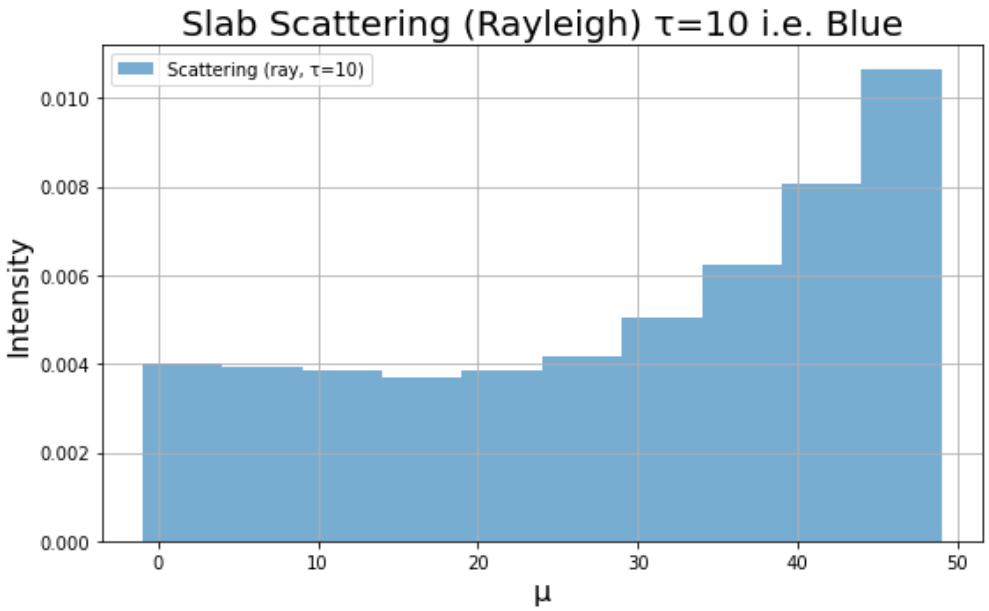


Figure 4: Rayleigh scattering with $\tau = 10$: Intensity is strongly forward and backward peaked due to the $1 + \cos^2 \hat{\theta}$ phase function and high optical depth. Blue photons are more likely to scatter, and most observed photons come from directions away from the Sun.

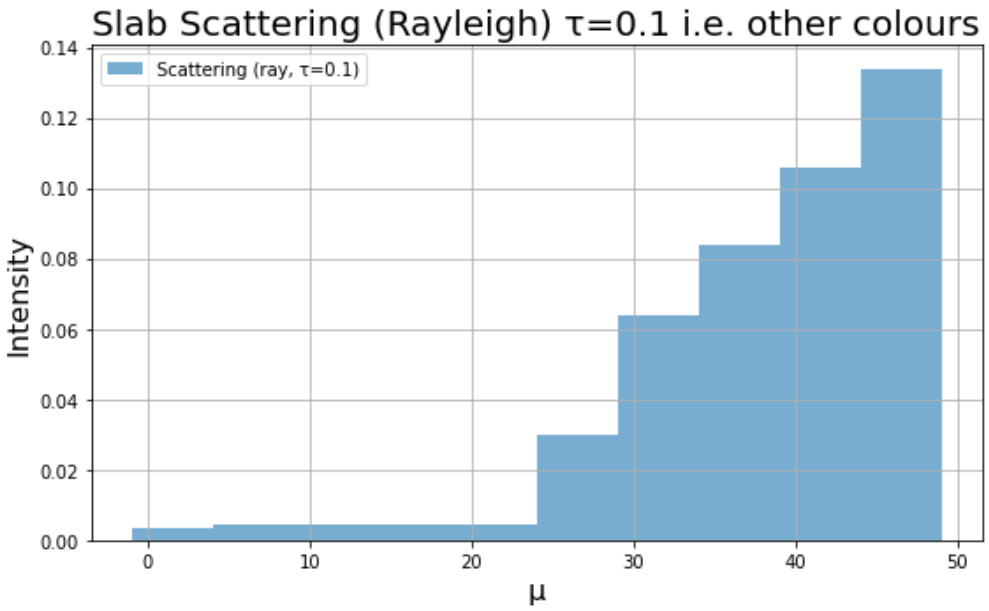


Figure 5: Rayleigh scattering with $\tau = 0.1$: The slab is optically thin, so fewer scattering events occur. Intensity is more uniformly distributed across directions, mimicking how redder wavelengths (which scatter less) are less affected by the atmosphere.

**Why the sky is blue:** These results provide a simplified explanation of why the sky is blue. Blue photons (shorter wavelength) experience stronger Rayleigh scattering and, in an optically thick atmosphere ($\tau = 10$), are scattered multiple times before reaching the observer — mostly from directions away from the Sun. This explains the diffuse blue appearance of the sky when not looking directly at the Sun. Redder photons (with

lower scattering cross-sections) are less affected in thinner atmospheres ($\tau = 0.1$), which is why sunsets appear red: blue light has already been scattered out of the line of sight.

## Terminal Output Summary

The terminal output below confirms the performance of both sampling methods and the photon transport simulations:

- **Rejection Sampling:** 66.69% efficiency, runtime 0.273 seconds.
- **Inverse Transform Sampling:** 100.00% efficiency, runtime 0.107 seconds.
- **Photon Transport:** No photons were absorbed in any simulation. All photons either scattered or escaped, as expected given the albedo $a = 1$.

```
Rejection Sampling Efficiency: 66.69%
Time: 0.273 s

Inverse Transform Sampling Efficiency: 100.00%
Time: 0.107 s
Simulated tau=10.0, method=iso → tau_10.0_iso.txt | Absorbed: 0 (0.00%)
Simulated tau=10.0, method=ray → tau_10.0_ray.txt | Absorbed: 0 (0.00%)
Simulated tau=0.1, method=ray → tau_0.1_ray.txt | Absorbed: 0 (0.00%)
```

Figure 6: Terminal output displaying the sampling efficiencies, runtimes, and photon absorption statistics for each simulation.